Geol Rundsch (1997) 86:141–155

ORIGINAL PAPER

F. Hauff · K. Hoernle · H.-U. Schmincke
R. Werner

A Mid Cretaceous origin for the Galápagos hotspot: volcanological, petrological and geochemical evidence from Costa Rican oceanic crustal segments

Received: 29 July 1996 / Accepted: 22 September 1996

Abstract The Quepos, Nicoya and Herradura oceanic igneous terranes in Costa Rica are conspicuous features of a Mid to Late Cretaceous regional magmatic event that encompasses similar terranes in Central America, Colombia, Ecuador and the Caribbean. The Quepos terrane (66 Ma), which consists of ol-cpx phyric, tholeiitic pillow lavas overlain by highly vesicular hyaloclastites, breccias and conglomerates, is interpreted as an uplifted seamount/ocean island complex. The Nicoya (~90 Ma) and Herradura terranes consist of fault-bounded sequences of sediments, tholeiitic volcanics (pillow lavas and massive sheet flows) and plutonic rocks. The volcanic rocks were emplaced at relatively high eruption rates in moderate to deep water, possibly forming part of an oceanic plateau. Major and trace element data from Nicoya/Herradura tholeiites indicate higher melting temperatures than inferred for normal mid-ocean-ridge basalts (MORB) and/or a different source composition. Sr–Nd–Pb isotopic ratios from all three terranes are distinct from MORB but resemble those from the Galápagos hotspot. The volcanological, petrological and geochemical data from Costa Rican volcanic terranes, combined with published age data, paleomagnetic results and plate tectonic reconstructions of this region, provide strong evidence for a Mid Cretaceous (~90 Ma) age for the Galápagos hotspot, making it one of the oldest known, active hotspots on Earth. Our results also support an origin of the Caribbean Plate through melting of the head of the Galápagos starting plume.

F. Hauff (✉) · K. Hoernle · H.-U. Schmincke · R. Werner
Department of Volcanology and Petrology, GEOMAR,
Wischhofstr. 1-3, D-24148 Kiel, Germany
Fax: (49) 431-600-2978
E-mail: fhauff@geomar.de

Key words Costa Rica · Ophiolites · Oceanic crust · Hotspot · Galápagos islands · Volcanology · Petrology · Geochemistry · Isotopes

Introduction

The origin, age and emplacement of numerous uplifted oceanic crustal segments along the Pacific Coast of Central America (Fig. 1) is a matter of ongoing debate, with models of in situ formation contrasting with models of terrane accretion. Age estimates of these complexes range from Jurassic to Paleocene (Schmidt-Effing, 1979). The term ophiolite is commonly used for these complexes, but we prefer oceanic igneous terranes because 1) crucial portions of the ophiolite inventory (Coleman, 1977), such as a sheeted dike complex, are generally missing and 2) the segments occur as fault-bounded blocks of different ages. At least six such terranes are exposed along the Pacific coast in Costa Rica: Santa Elena Peninsula, Nicoya Peninsula, Herradura, Quepos, Osa Peninsula, Golfito and Burica Peninsula (Fig. 1). Here we integrate volcanological, petrological and geochemical data from the Nicoya, Herradura and Quepos terranes in order 1) to assess the petrogenesis of the igneous suites and 2) to determine the origin of the convergent plate margin of Costa Rica.

A wide variety of models have been proposed for the origin of the Central American oceanic terranes. Their present location at a convergent plate margin have led some workers to favour accretion of Pacific crust (Galli-Olivier, 1979), while others prefer uplift of in situ Caribbean basement (Donnelly et al., 1990). More complex, multistage geotectonic models based on biostratigraphic and geochemical studies invoke terrane formation at a mid-ocean ridge (north Nicoya) and subsequent overprinting in intra-plate and primitive island arc settings (south Nicoya, Herradura, Osa) (Schmidt-Effing, 1979; Frisch et al., 1992). Still others

have used plate tectonic reconstructions to show that the Central American igneous terranes, as well as the Caribbean Igneous Province, could have formed from the Galápagos hotspot (Flüh, 1983; Duncan and Hargraves, 1984). Additional support for an intra-plate origin comes from the field observations and trace element data from the Quepos terrane (Frisch et al., 1992). Nevertheless, a direct link to the Galápagos hotspot through petrological or geochemical studies has yet to be established. In the absence of such evidence, a possible Galápagos origin for Costa Rican terranes (>65 Ma) and the Caribbean Igneous Province (~90 Ma) is highly speculative, considering the large age span (~55 Ma) between the terranes and the oldest part of the Galápagos hotspot track off the coast of Costa Rica (~10 Ma, von Huene, pers. com. 1995).

In this study, field observations and volcanological data are used to constrain the paleoenvironment of these terranes. New major element, trace element and Sr-Nd-Pb isotopic data on fresh glasses and hand-picked chips from whole-rock samples are evaluated with emphasis on fractionation histories, melting conditions and source characteristics. A petrogenetic model for the origin of the oceanic crustal segments is presented and implications for the origin and evolution of the Caribbean plate are discussed.

Analytical methods

The freshest possible material was sampled and care was taken to cover the entire rock spectrum. Samples were crushed to 0.5–1 cm size and then cleaned with distilled water. Whole-rock chips free of veins, as well as fresh glass particles, were carefully selected under a binocular microscope. Chips were ground to rock flour in an agate mortar or mill. H_2O and CO_2 were determined with a Rosemount Infrared Photometer CSA 5003. Bulk rock analyses of major and trace (Cr, Ni, Sr, Ba, Zr, Y shown in Table 1a) elements were performed on fused beads (flux/sample ratio = 6:1) with a Philips X'unique PW 1480 X-ray fluorescence spectrometer (XRF). Iron is measured as ferric iron ($Fe_2O_3{}^t$) and reported as total ferrous iron ($FeO^* = 0.89 \times Fe_2O_3{}^T$. Hawaiian basalt standard BHVO-1 was prepared and analyzed with the samples in order to evaluate precision and accuracy of the analyses (Table 1a). Accuracy for major elements is generally within $\pm 3\%$ of the working values of (Govindaraju, 1994) except for Na_2O ($\pm 7\%$). Sr, Y, Cr and Ba are within $\pm 4\%$ and Ni, Zr within 10% of the recommended values.

Major element compositions and volatile contents (e.g. S, Table 1b) of basaltic glasses were determined using a CAMECA SX 50 electron microprobe (EMP). Operating conditions were 15 kV accelerating voltage and 10 nA for the beam current with a beam size of 9×4 μm. Data for glass shards (Table 1b) represent an average of 25 analysed points per shard. The natural glass standard JDF-D2 and the mineral standard PLAG were used for calibration.

Additional trace elements (Rb, Pb, Th, U, Nb, Ta, Hf and all REE, Table 1a) were analysed with a VG Plasmaquad PQ1-ICP-MS (Inductively Coupled Plasma-Mass Spectrometry) at the Geological Institute, University of Kiel after the methods of (Garbe-Schönberg, 1993).

Sr, Nd and Pb isotopic compositions of glass and whole rock separates were determined by thermal-ionisation mass spectrometry (TIMS) using a Finnigan MAT261 mass spectrometer at the Department of Geological Sciences, University of California, Santa Barbara. Analytical techniques used are described in (Hoernle and Tilton, 1991) and (Hoernle et al., 1991). Hand-picked glass separates were leached in cold 3N HNO_3 for 20 minutes in an ultrasonic bath, whereas whole-rock powders were leached with a hot mixture of 50% 6N HCl and 50% 8N HNO_3 for 45 minutes. The measured $^{87}Sr/^{86}Sr$ ratio was normalized within-run to $^{86}Sr/^{88}Sr = 0.1194$ and then adjusted to a $^{87}Sr/^{86}Sr$ value of 0.710235 for NBS987. The $^{143}Nd/^{144}Nd$ ratio was normalized within-run to $^{146}Nd/^{144}Nd = 0.721900$ and then adjusted to a $^{143}Nd/^{144}Nd$ value of 0.511850 for the La Jolla standard. $^{87}Sr/^{86}Sr$ ratios were measured in static mode and $^{143}Nd/^{144}Nd$ ratios in dynamic mode. The Pb isotope data are corrected for 0.125% mass fractionation per atomic mass unit.

Accurate determination of initial isotope ratios is often difficult in altered rocks. The leaching techniques described above have been shown to minimize the effects of alteration on the Sr, Nd and Pb isotopic compositions of basalts from marine environments (Hoernle and Tilton, 1991). Nevertheless, parent/daughter ratios, especially Rb/Sr and U/Pb, are also susceptible to alteration, due to the mobility of Rb, Sr and U in hydrous fluids. Therefore, we undertook the following measures to aid in the determination of initial Sr and Pb isotope ratios. 1) We used Rb/Sr from the freshest samples (LOI < 1.6 wt%) from each region. 2) We determined the U/Pb ratio independently using Nb and Ce data (Table 2), since both of these elements are relatively immobile during seawater alteration and the Nb/U (47 ± 10) and Ce/Pb (25 ± 5) ratios are considered to be relatively uniform in mantle-derived rocks (Hofmann et al., 1986; although some exceptions exist, e.g. Hoernle and Schmincke, 1993; Hémond et al., 1994). The U/Pb ratios calculated from Nb and Ce concentrations fall within the range of those measured directly but show less variation, suggesting that they may be more accurate. In conclusion, the correction for in situ decay for all five isotope systems is relatively minor (Table 2).

Field relationships and volcanology

The Quepos terrrane contains a wide spectrum of volcanic and pyroclastic rocks (Fig. 2). The lowermost exposed stratigraphic unit comprises ol-cpx phyric pillow basalts and pelagic, foraminiferous chalk, which yields a biostratigraphic age of 66 Ma (Baumgartner et al., 1984). The basal unit is overlain by a thick (50–100 m) volcaniclastic series. In this series, hyaloclastites, containing highly vesicular ash and lapilli particles interlayered with thin lava flows, are overlain by breccias, debris flows and conglomerates. These volcaniclastic deposits appear to have formed the flank of a volcanic edifice. The presence of vesicular lapilli and oxidized pebbles provides clear evidence for shallow marine to subaerial eruptions. Plutonic rocks within the breccias and debris flows indicate erosion of deep-seated parts of the Quepos complex. We interpret the entire stratigraphic section as a seamount that emerged above sea level and formed an ocean island, consistent with the interpretation of (Frisch et al. 1992).

After magmatic activity ceased, erosion and subsidence (possibly as a result of lithospheric thermal relaxation) resulted in the drowning of the volcanic edifice.

Table 1a Representative major and trace element analyses of whole rocks (w.r.) for Nicoya, Herradura and Quepos. FeO* is total iron as ferrous iron. The rare earth elements (REE) and elements marked with an * were measured by ICP-MS. All other elements and oxides are determined by XRF. Sample AN3 and AN110 are from north Nicoya, AN53 and AN86 from south Nicoya. AH = Herradura; AQ = Quepos

Sample	AN3 w.r.	AN110 w.r.	AN53 w.r.	AN86 w.r.	AH1b w.r.	AQ66 w.r.	AQ16 w.r.	AQ19 w.r.	AQ72 w.r.	BHVO-1 n = 10	BHVO-1 2σ
Major elements (*wt %*)											
SiO_2	48.1	49.4	49.4	49.8	49.3	48.0	47.2	47.8	48.7	49.75	0.17
TiO_2	1.65	1.02	0.99	2.43	1.06	2.89	2.28	2.73	2.22	2.78	0.01
Al_2O_3	13.32	14.01	14.36	13.07	14.36	13.64	13.05	13.84	13.81	13.56	0.07
FeO*	13.20	10.71	10.48	13.85	10.45	11.45	11.59	11.23	10.53	12.33	0.05
MnO	0.232	0.198	0.229	0.233	0.171	0.185	0.178	0.188	0.151	0.17	0.00
MgO	6.68	8.38	8.48	5.58	8.41	6.83	8.66	7.21	6.26	7.14	0.05
CaO	10.84	11.94	12.47	8.78	11.94	10.43	10.99	11.02	9.93	11.27	0.04
Na_2O	2.11	1.81	1.84	2.68	1.79	2.80	2.24	2.52	4.33	2.09	0.06
K_2O	0.20	0.09	0.04	0.14	0.05	0.48	0.24	0.39	0.14	0.52	0.01
P_2O_5	0.133	0.069	0.069	0.221	0.081	0.261	0.176	0.244	0.200	0.27	0.01
H_2O	2.29	1.79	0.95	1.35	1.68	1.02	1.39	1.22	2.57	0.21	0.01
CO_2	0.08	0.16	0.13	0.09	0.13	0.05	0.11	0.12	0.09	0.04	0.00
Total	100.6	99.6	99.5	100.0	99.4	99.5	99.6	99.9	100.3	100.13	0.29
Trace elements (*ppm*)											
Cr	77	311	228	68	394	304	750	338	201	290.18	4.54
Ni	78	117	142	77	128	142	303	162	96	132.88	8.38
Y	37	25	24	46	22	32	26	33	30	28.35	1.41
Zr	96	57	54	148	53	174	123	165	119	159.18	4.75
Hf*	2.49	1.37	1.27	3.75	1.33	4.29	3.20	4.24	3.17	4.27	0.07
Nb*	5.64	3.01	2.97	8.83	4.02	16.7	12.4	16.3	12.2	19.03	0.26
Ta*	0.46	0.18	0.18	0.55	0.40	1.02	0.88	1.11	0.81	1.18	0.03
Rb*	3.62	1.05	0.33	1.21	0.99	4.97	2.74	5.88	2.54	9.51	0.15
Sr	114	105	75	100	90	295	218	272	286	398.35	3.20
Ba	<8	32	14	52	22	85	35	60	<8	145.12	11.81
Pb*	0.490	0.216	0.347	0.804	0.396	1.171	0.580	0.840	0.790	2.26	0.18
Th*	0.356	0.247	0.242	0.748	0.305	1.448	0.720	1.020	0.810	1.15	0.03
U*	0.121	0.059	0.078	0.237	0.090	0.463	0.230	0.310	0.380	0.40	0.01
La	4.77	2.32	2.32	5.98	2.87	12.90	8.58	12.06	10.43	15.87	0.32
Ce	12.47	6.45	6.45	18.24	7.68	33.03	21.43	30.17	24.44	37.71	0.10
Pr	1.93	0.98	0.98	2.76	1.11	4.48	3.12	4.37	3.48	5.16	0.10
Nd	9.80	5.16	5.16	14.01	5.75	20.73	14.62	20.00	16.47	23.46	0.01
Sm	3.36	1.82	1.79	4.62	1.85	5.51	3.99	5.47	4.34	5.85	0.03
Eu	1.20	0.69	0.68	1.57	0.71	1.84	1.40	1.82	1.52	1.93	0.04
Gd	4.43	2.42	2.38	5.93	2.47	5.85	4.45	6.08	5.14	6.01	0.07
Tb	0.79	0.45	0.45	1.09	0.45	0.94	0.73	0.94	0.83	0.90	0.02
Dy	5.09	3.06	3.04	7.34	3.07	5.68	4.25	5.50	4.91	4.95	0.08
Ho	1.09	0.67	0.67	1.58	0.66	1.09	0.83	1.08	1.01	0.93	0.01
Er	3.16	1.94	1.94	4.53	1.94	2.90	2.27	2.92	2.76	2.44	0.04
Tm	0.46	0.28	0.28	0.66	0.28	0.39	0.30	0.39	0.38	0.32	0.01
Yb	3.09	1.90	1.92	4.53	1.94	2.43	1.86	2.48	2.44	1.93	0.05
Lu	0.46	0.29	0.29	0.67	0.29	0.35	0.27	0.34	0.35	0.27	0.00

Table 1b Representative glass analyses by EMP. Samples AN3 and AN7 are from north Nicoya and AN40 is from south Nicoya

Sample	AN3 glass	AN7 glass	AN40 glass
Major elements (wt%)			
SiO_2	50.7	49.9	51.9
TiO_2	1.63	2.69	1.30
Al_2O_3	13.40	12.54	13.68
FeO*	13.78	16.43	12.41
MnO	0.236	0.248	0.201
MgO	6.31	4.83	6.87
CaO	10.89	9.50	11.24
Na_2O	2.12	2.57	1.92
K_2O	0.13	0.23	0.09
P_2O_5	0.071	0.195	0.033
SO_2	0.30	0.40	0.22
Total	99.5	99.5	99.9

The resulting seamount was buried by Eocene turbidites (Baumgartner et al., 1984) from the Central American Arc and was subsequently accreted to the fore arc. The indented Pacific continental margin of Costa Rica shows abundant evidence for recent subduction of seamounts in this region (Huene et al., 1995; Hinz et al., 1996).

The tectonically dismembered Nicoya and Herradura terranes consist of volcanic and plutonic rocks associated with siliciclastic, carbonate and minor volcaniclastic sediments (Fig. 2). Biostratigraphic ages reported for radiolarite sequences range from Jurassic to Early Cretaceous (Schmidt-Effing, 1979; Gursky, 1994). Since the contacts between sediments and volcanic rocks are tectonic or intrusive, the radiolarite ages do not necessarily represent the formation age of the igneous suite. Whole-rock K-Ar studies carried out on the Nicoya Peninsula yield a large age spectrum (46–72 Ma; Alvarado et al., 1992), which most likely reflects Ar loss during alteration or thermal resetting. Evidence for the formation of the Nicoya igneous suite around 90 Ma comes from Cenomanian/Turonian (91 Ma) intrapillow sediments in south Nicoya (Tournon, 1984) and an Ar–Ar plateau age of 88.2 ± 3.1 Ma obtained on a basalt from north Nicoya (Sinton et al., 1993).

Pillow lavas and massive basalt flows are common throughout Nicoya and Herradura. Lack of vesicularity in most lavas and high sulfur concentrations (1000–2000 ppm S; Table 1b) of fresh glasses from pillow rims indicate low degrees of degassing and therefore eruption in moderate to deep water (Moore and Schilling, 1973). The thickness of cooling units (up to 50 m) and the lack of primary sediment intercalations suggests high eruption rates over relatively short time intervals. Intrusive rocks (primarily tholeiitic gabbros and plagiogranites) are only exposed in north Nicoya. Although most contacts between intrusive and extrusive or sedimentary sequences are tectonic, some outcrops showed clear intrusion of gabbro into pillow and radiolarian sequences, for example north of Palya Flamingo. Therefore at least some of the plutonic rocks postdate the volcanic and sedimentary sequences.

Table 2 Measured isotope ratios of glasses and whole rocks from Nicoya, Herradura and Quepos. For locations and major and trace element compositions see Table 1a and Table 1b. Initial isotope ratios were calculated using trace element data in Table 1. For example AN3 (wr.) is from the pillow interior and AN3 from the glassy pillow rim. Initial Pb isotopic ratios indicated with an * are calculated using Ce/Pb of 25 and Nb/U of 47 from Hofmann et al. (1986)

Sample Age (Ma)	AN3 glass 90	AN40 glass 90	AH1b w.r. 90	AQ66 66	AQ72 66
$^{87}Rb/^{87}Sr$	0.080	0.025	0.008	0.063	0.023
$^{87}Sr/^{86}Sr$	0.703173 (15)	0.7037981 (11)	0.703211 (13)	0.703385 (15)	0.703937 (15)
$^{87}Sr/^{86}Sr$ in	0.703070	0.703765	0.703200	0.703326	0.703915
$^{147}Sm/^{144}Nd$	0.206	0.202	0.194	0.160	0.159
$^{143}Nd/^{144}Nd$	0.513018 (8)	0.512997 (9)	0.513031 (7)	0.512977 (5)	0.512940 (6)
$^{143}Nd/^{144}Nd$ in	0.512896	0.512878	0.512917	0.512908	0.512872
$^{238}U/^{204}Pb$	16	26	13	26	31
$^{238}U/^{204}Pb$*	15	16	20	19	17
$^{232}Th/^{204}Pb$	48	62	45	82	68
$^{232}Th/^{204}Pb$*	47	46	72	80	55
$^{232}Th/^{238}U$	3.0	2.4	3.5	3.2	2.2
$^{232}Th/^{238}U$*	3.7	2.8	3.7	4.2	3.2
$^{206}Pb/^{204}Pb$	19.187 (2)	19.236 (4)	19.599 (8)	19.322 (3)	19.296 (2)
$^{206}Pb/^{204}Pb$ in	18.964	18.871	19.418	19.060	18.979
$^{206}Pb/^{204}Pb$ in*	18.970	19.005	19.321	19.127	19.120
$^{207}Pb/^{204}Pb$	15.550 (2)	15.563 (3)	15.587 (8)	15.569 (3)	15.574 (2)
$^{207}Pb/^{204}Pb$ in	15.540	15.546	15.579	15.557	15.560
$^{207}Pb/^{204}Pb$ in*	15.540	15.553	15.574	15.560	15.566
$^{208}Pb/^{204}Pb$	38.742 (5)	38.886 (8)	39.192 (25)	38.887 (8)	38.721 (4)
$^{208}Pb/^{204}Pb$ in	38.526	38.610	38.991	38.618	38.498
$^{208}Pb/^{204}Pb$ in*	38.530	z38.680	38.867	38.67	38.542

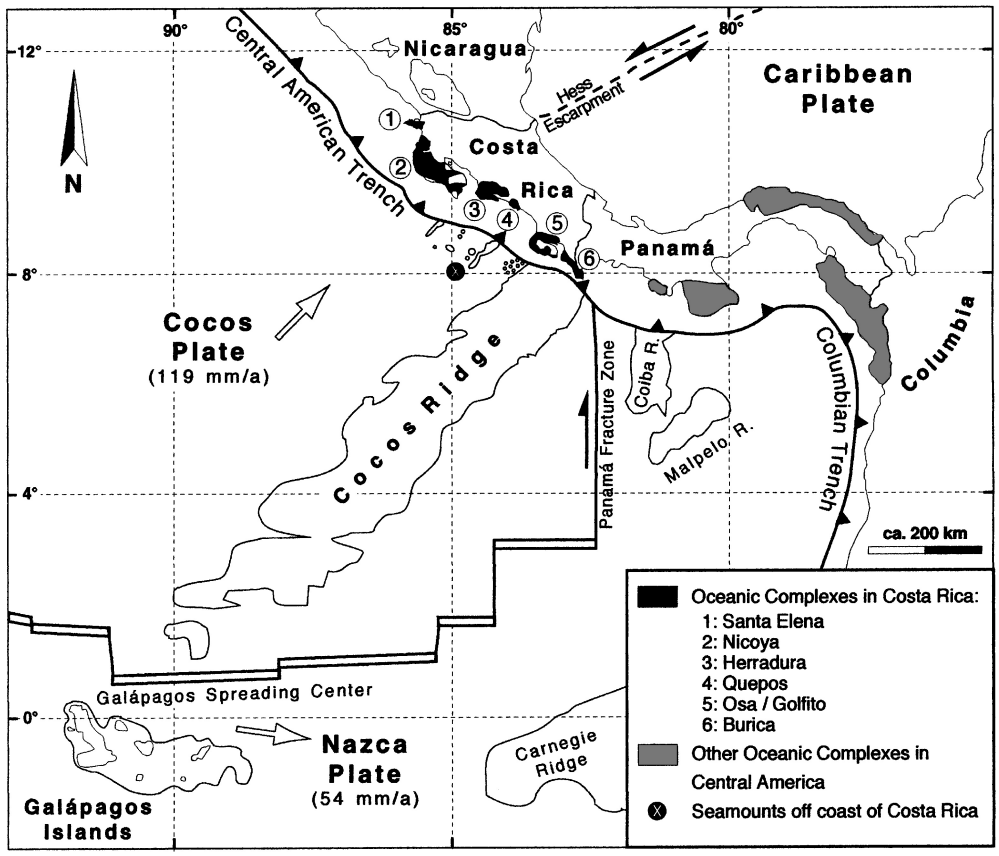

Fig. 1 Geologic map of Central America and the Eastern Pacific after (Mann 1995). Areas with ophiolite characteristics crop out along the convergent plate margin between the Caribbean and Pacific plates. Presently the Cocos Ridge, representing part of the Galápagos hotspot track, and associated seamounts are being subducted or accreted along the Central American trench

Petrography and analytical results

The volcanic rocks of Nicoya and Herradura are generally aphyric and range from coarse-grained dolerites in massive flows to fine grained pillow lavas. The groundmass consists of plagioclase (plag) and clinopyroxene (cpx) with minor olivine (ol). Chlorite and thin calcite veins are ubiquitous. Basaltic rocks from Quepos contain ol and cpx phenocrysts but rarely plag. The groundmass is often very fine grained and contains plag and cpx.

Volcanic rocks from Nicoya and Herradura are tholeiitic with $SiO_2 = 50–52$ wt% and MgO = 3.5–9.1 wt% (Table 1a and 1b). Most whole-rock samples (85%) have H_2O contents of 1–2.5 wt% and $CO_2 < 0.2$ wt%. Good correlations exist between MgO and elements thought to be immobile (Fig. 3a, b). Even the most mobile elements (e.g. Na, K, Ba) generally show good correlations with MgO when glass analyses or the freshest whole rock samples (LOI < 1.6 wt%) are considered (Fig. 3c). No differences in major and trace element composition are observed between north and south Nicoya. The Herradura basalts have remarkably similar major and trace elements contents to Nicoya tholeiites at similar MgO content (Fig. 3a). As MgO decreases, CaO, Al_2O_3, Ni Cr and Eu/Eu* decrease, but FeO* (total iron as FeO) and incompatible elements (e.g. Ti, P, Zr, Y, REE, Ba, Pb, U, Th) increase (Fig. 3 and 6), consistent with low pressure fractionation of phases present in the groundmass (ol, plag ± Cr-spinel) at pressures < 5 kb (Albarede and Tamagnan, 1988).

Incompatible element abundances for the most mafic (MgO = 8.5 wt%) Nicoya and Herradura rocks, normalized to primitive mantle, form relatively flat patterns on multi-element diagrams with relative depletions in K, U, Th, Ba and Rb but slight enrichments in Pb (Fig. 4). Although the patterns show similarities to MORB, the Costa Rican rocks generally have lower abundances of K and all elements from Pr through Lu (Figs 4, 7). Characteristic peaks at Ba, K, Sr and troughs at Nb-Ta and La-Ce observed in subduction zone tholeiites are absent from Nicoya and Herradura samples. The trace element patterns of Nicoya and Herradura however are characteristic of oceanic plateaus or Large Igneous Provinces, such as Ontong Java and the Caribbean Plate (Kerr et al., 1996a and references therein).

Quepos transitional tholeiites (henceforth simply referred to as tholeiites) have $SiO_2 = 48–51$ wt% and MgO = 5.9–8.9 wt%. As MgO decreases, CaO, Cr and Ni also decrease but Al_2O_3 and incompatible element (e.g. Ba, Sr) concentrations increase (Fig. 3b, c, 6). These

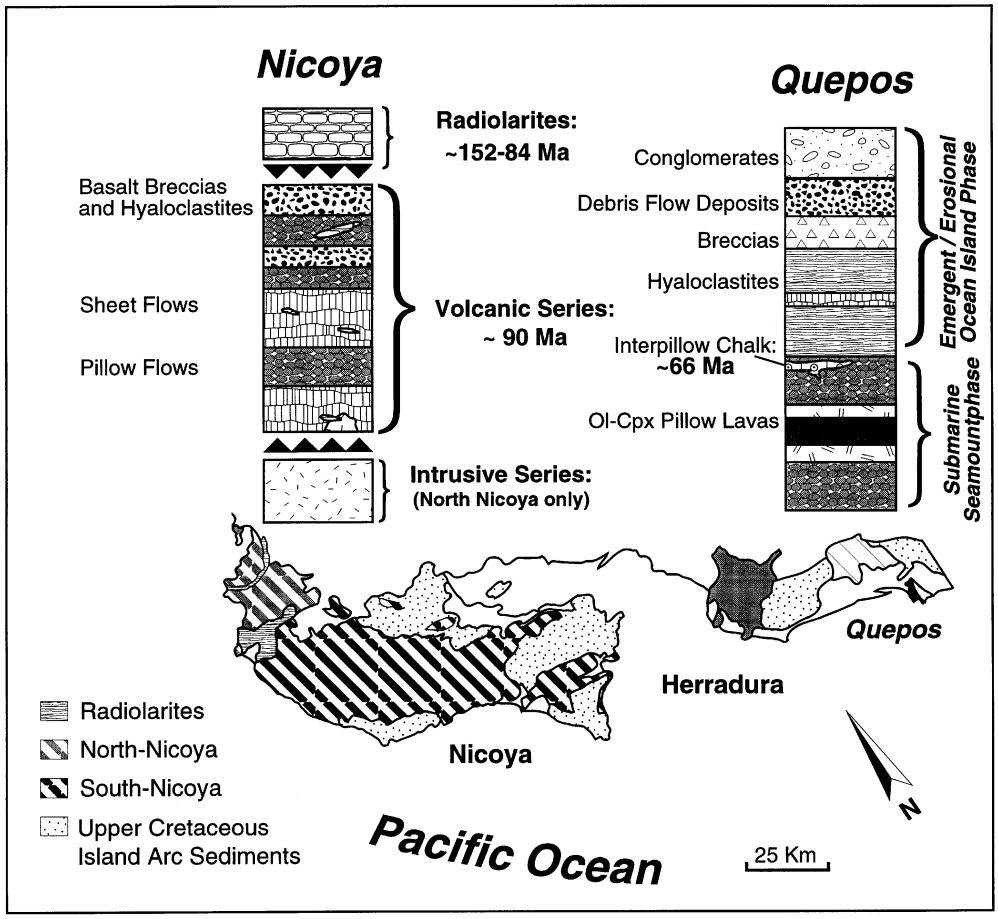

Fig. 2 Lithostratigraphic columns and simplified geologic map (after Frisch et al., 1992) of the Quepos and Nicoya oceanic igneous complexes are shown. The heterogeneous rock sequence of Quepos (66 Ma) is interpreted as the submarine shield phase, followed by an emergent/erosional phase, of an ocean island. Fault-bounded sequences of radiolarites and extrusive and intrusive rocks are constituents of the Nicoya basement. Primary sedimentary contacts only exist between lava flow units. No differences in volcanic facies were observed between north and south Nicoya. The probable formation age of ~90 Ma is based on lithostratigraphic ages from intra-pillow sediments and an $^{40}Ar/^{39}Ar$ whole rock age data (see text for references). The minimum age for Nicoya/Herradura comes from Upper Cretaceous (75 Ma) sediments from the Central American Arc, which overlie the terranes

chemical variations are consistent with fractionation of the observed phenocryst phase (Ol, Cpx ± Cr-Spinel) at pressures > 5 kb (Albarede and Tamagnan, 1988). Near constant Eu/Eu* (1.01–0.95), decreasing CaO/Al_2O_3 and increasing Sr with decreasing MgO argue against significant plagioclase fractionation. Relative to primitive Nicoya and Herradura tholeiites, Quepos tholeiites are significantly enriched in all incompatible elements (Fig. 4), with the degree of enrichment increasing with incompatibility (i.e. from right to left in Fig. 4). The most incompatible elements are enriched by a factor of six in Quepos tholeiites. The Quepos incompatible element pattern is strikingly similar to those from ocean islands with HIMU-type (high mu = $^{238}U/^{204}Pb$) isotopic characteristics, such as St. Helena (see Fig. 4).

Measured and initial Nd and Pb isotopic ratios from all three regions are relatively uniform: $^{143}Nd/^{144}Nd$: measured = 0.51294–303, initial = 0.51287–92; $^{206}Pb/^{204}Pb$: measured = 19.2–19.6, initial = 19.0–19.3; $^{207}Pb/^{204}Pb$: measured = 15.55–9, initial = 15.54–7; $^{208}Pb/^{204}Pb$: measured = 38.7–39.2, initial = 38.5–39.0 (Table 2). Nd and Pb isotopic ratios are nearly within 2σ errors for Quepos and Nicoya, whereas Herradura rocks have slightly more radiogenic Pb. In contrast, Sr isotopic ratios span a fairly broad range ($^{87}Sr/^{86}Sr$: measured = 0.7032–9; initial = 0.7031–9), yet overlap for all three regions. An increase in Sr isotopic ratio in whole rock sample AQ72 ($^{87}Sr/^{86}Sr$ = 0.7039) due to sea water alteration cannot be ruled out. The relatively high $^{87}Sr/^{86}Sr$ (0.7038) for fresh glass from sample AN40, however, suggests that it could reflect the magmatic composition. The narrow range in Nd and Pb isotope ratios and the similarities in Sr isotopic ratios for the rocks from each region indicate that volcanic rocks from all three areas could be derived from a common source, despite their age differences. This potential mantle source is distinct from all known MORB, because Pb isotopes are more radiogenic than in Pacific and Indian MORB and Nd isotopes are generally less radiogenic than in Pacific and Atlantic MORB. The Sr, Nd and Pb isotope ratios, however, are within the broad compositional range of oceanic island basalts, which are commonly thought to be associated with plume-type volcanism and fall within the field of the Galápagos Islands, the closest hotspot (Fig. 10a, b).

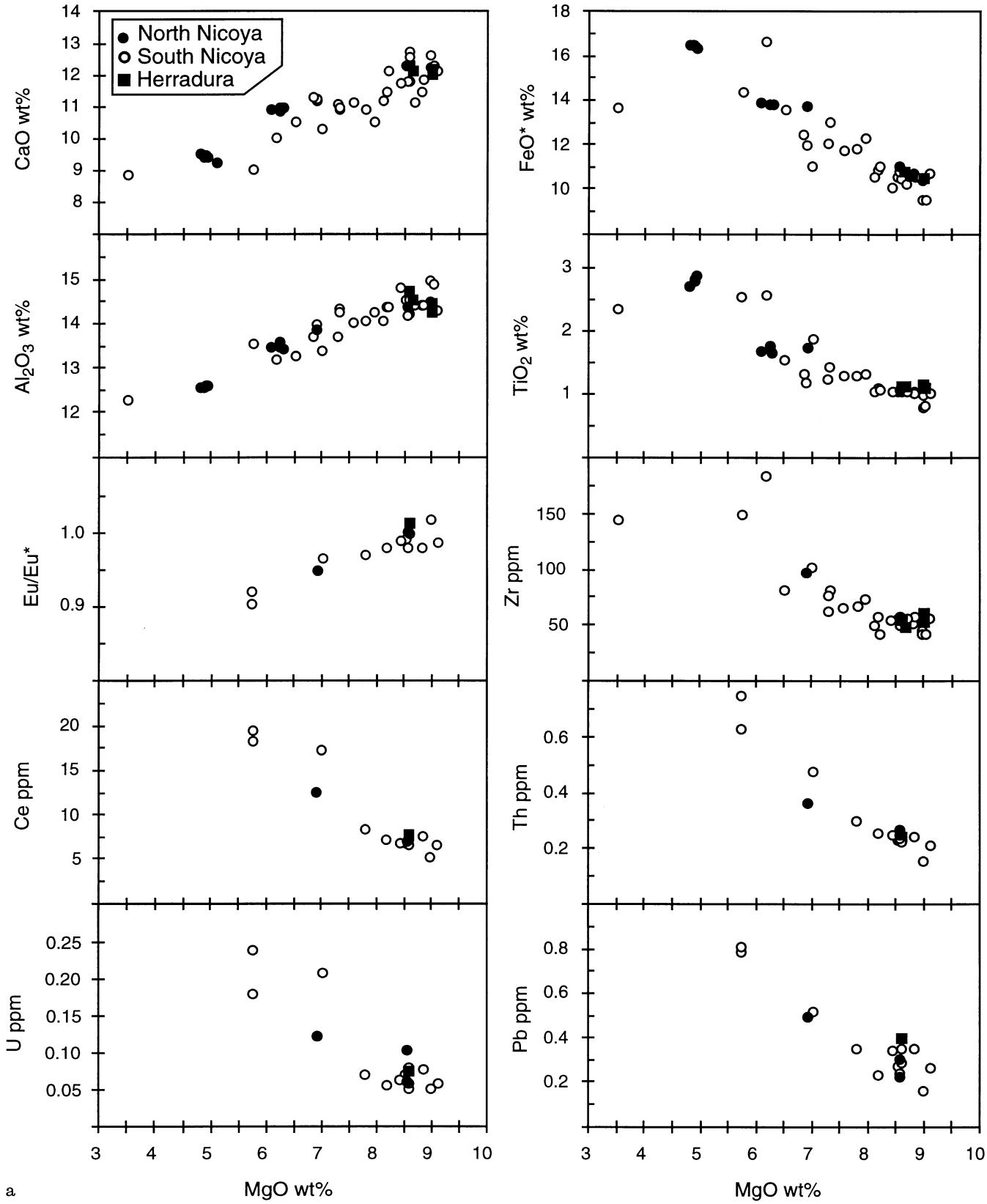

Fig. 3a Representative major and trace element data for Nicoya and Herradura tholeiites, plotted against MgO. Size of Europium anomaly on REE diagram is calculated as follows: $Eu/Eu^* = \sqrt{Eu_N/(Sm_N \times Gd_N)}$, element concentrations are chondrite-normalized (N)

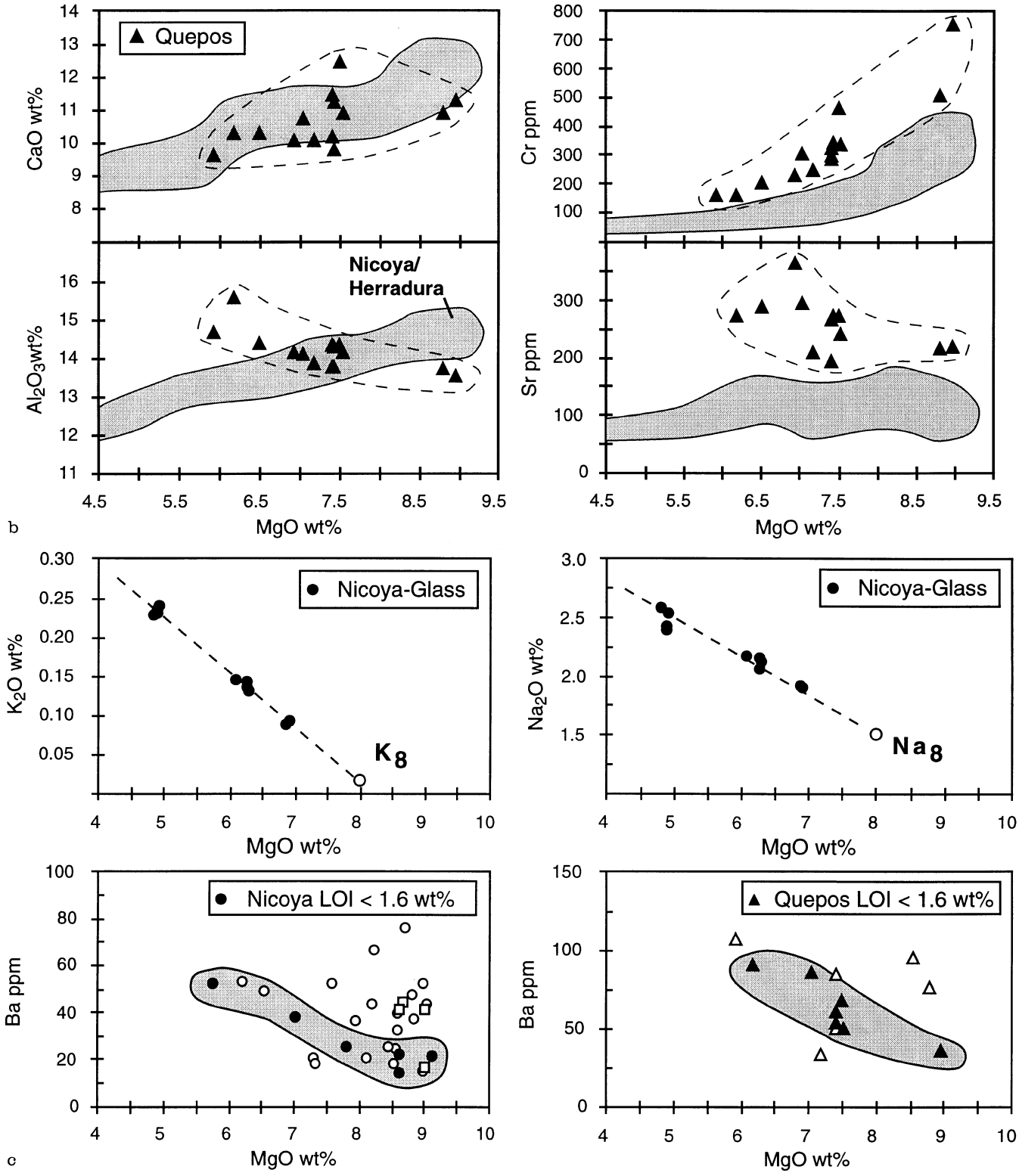

Fig. 3b Representative major and trace elements of Quepos tholeiites against MgO. Data for Nicoya/Herradura tholeiites (shaded fields) are also shown. In contrast to Nicoya tholeiites, Al_2O_3 and Sr increase with decreasing MgO, which indicates clinopyroxene instead of plagioclase fractionation. **c** Correlations of representative mobile elements with MgO for Nicoya and Quepos tholeiites. K and Na concentrations were obtained from fresh glasses by electron microprobe analyses. K_8 (K at MgO = 8) and Na_8 (Na at MgO = 8) are obtained after Klein and Langmuir (1987). Samples with < 1.6 wt% LOI are indicated as filled symbols on plots of Ba and Sr vs. MgO. Open symbols have LOI > 1.6 wt%

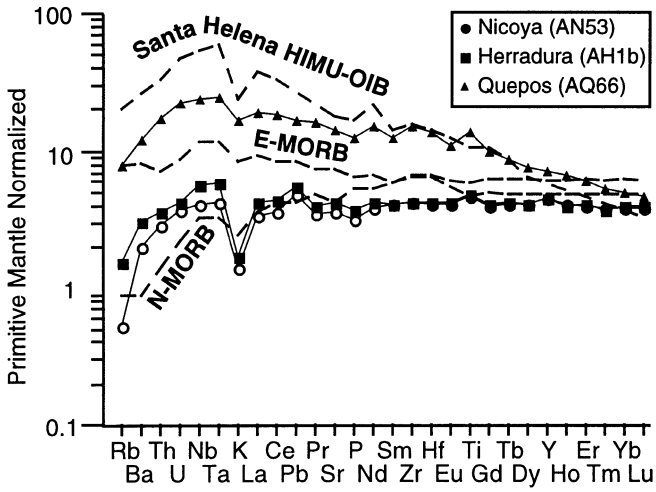

Fig. 4 Primitive mantle normalized multi-element diagram for representative Nicoya, Herradura and Quepos tholeiites (MgO = 7–9 wt%). Quepos tholeiites have higher abundances of all incompatible elements than Nicoya/Herradura tholeiites at similar MgO and have similar incompatible-element characteristics to basalts from HIMU ocean islands such as St. Helena (Chaffey et al., 1989). Average values for normal mid ocean ridge basalt (N-MORB) and enriched mid ocean ridge basalt (E-MORB) from Sun and McDonough (1989) are also shown

Discussion

Relationship between north Nicoya, south Nicoya and Herradura

Previous studies propose a complex, three-fold origin for the Nicoya Peninsula, which includes: 1) formation of the northern Nicoya complex at a Jurassic or older mid ocean ridge, 2) deposition of radiolarite sequences from Jurassic to Early Cretaceous, and 3) eruption of lavas in a primitive island arc and/or intra-plate setting to form the southern Nicoya complex in the Early Cretaceous (Schmidt-Effing, 1979; Frisch et al., 1992). The following observations, however, indicate a common region for the volcanic sequences across the entire Nicoya Peninsula: 1) the similarity of lava facies, 2) a common age of $\sim$90 Ma, 3) magmatic and tectonic contacts with radiolarite sequences, and 4) the similarity in major element, trace element and Nd-Pb isotopic geochemistry. The restriction of plutonic rocks to north Nicoya may reflect a local intrusive event or result from different levels of exposure within the same crustal block due to regional differences in uplift and/or tilt.

Support for a similar origin for the Herradura and Nicoya complexes comes from the remarkable similarity in volcanic facies and in major element, trace element and Sr-Nd isotope geochemistry. The differences in the Pb isotopic composition between the two regions may be an artefact of the small data set.

Differences in melting conditions for Nicoya/Herradura and Quepos tholeiites

Despite the differences in age, the similarity in Sr-Nd-Pb isotopic composition between the Nicoya/Herradura and Quepos terranes argue for derivation from a common source. Therefore differences in major and trace element abundances most likely reflect changes in the melting conditions between 90 Ma and 66 Ma. Below we evaluate the melting conditions for each area and explain the differences in the context of the melt column model.

Recent high-pressure, diamond aggregate melting experiments on spinel-lherzolite xenoliths indicate that SiO_2 contents in basaltic magmas are primarily controlled by pressure (depth) at which melting occurs rather than the degree of melting or source composition (Hirose and Kushiro, 1993). Primitive Quepos basalts have lower SiO_2 and Al_2O_3 but higher FeO* (Fig. 3b and 5) than the Nicoya and Herradura tholeiites, consistent with melting occurring at greater average depth for Quepos. Comparison with SiO_2 in the experimental results yields average depths of melting of $\sim$50 km for Quepos and of $\sim$35 km for Nicoya and Herradura, indicating that melting occurred primarily above the garnet stability field ($<$80 km). Further evidence that garnet was not a residual phase comes from the relatively flat chondrite-normalized heavy rare earth element (HREE) patterns, the relatively high HREE abundances and the absence of crossing HREE patterns for Quepos and Nicoya/Herradura at similar MgO (Fig. 9).

The melting experiments also show that MgO in primary melts correlates directly with melting temperature (Hirose and Kushiro, 1993). Primary MgO contents of Costa Rican tholeiites can be inferred on a plot of Ni vs. MgO (Fig. 6; Hart and Davis, 1978). Although Quepos tholeiites with 9 wt% MgO have Ni contents similar to primary melts, the most mafic Nicoya/Herradura tholeiites appear to have undergone $\sim$15% ol fractionation. Estimated MgO contents of 13 wt% for primary Nicoya/Herradura melts correlate with temperatures of 1380 $\pm$ 20 °C, whereas primary Quepos melts yield lower temperatures of 1280 $\pm$ 20 °C.

In accordance with the melt column except (e.g. Klein and Langmuir, 1987; Devey et al., 1994), the depth at which melting begins and ends will determine the length of the melting interval. The depth of melt initiation is controlled by the temperature of the upwelling mantle. Since lower melting temperatures are inferred for Quepos, melting must begin at shallower depth than for Nicoya and Herradura. The depth at which melting ends is controlled by the thickness of the lithosphere. Greater depths of fractional crystallization ($>$16 km) and greater average depth of melting despite lower average melting temperature require thicker lithosphere above the Quepos source. Shallower depth for the initiation of melting and greater depth for the

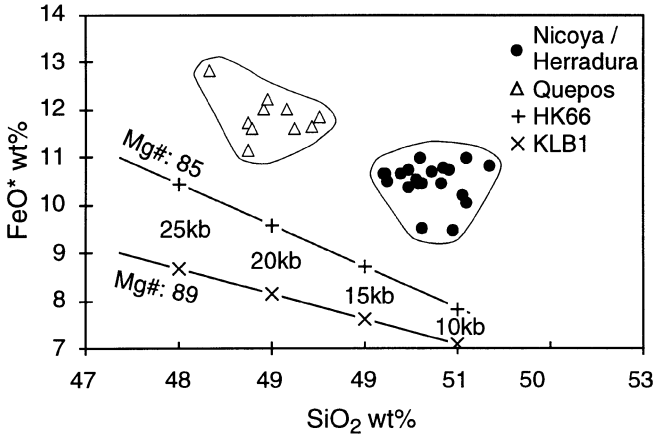

Fig. 5 SiO_2 versus FeO* (total iron as FeO) of tholeiites with MgO = 7–9 wt% from Nicoya, Herradura and Quepos. Also shown are fields for experimental results from spinel Iherzolite xenoliths HK66 with fo_{85} and KLB1 with fo_{90} (Hirose and Kushiro 1993). Pressure ranges (± 1.5 kbar) were calculated ($P = 195.88 + (-3.64 \times SiO_2)$, $R = 0.91$) from the experimental data. Costa Rican tholeiites have higher FeO* at a given SiO_2 content than produced in experiments suggesting derivation from a more iron-rich (fertile) source than used in the experiments

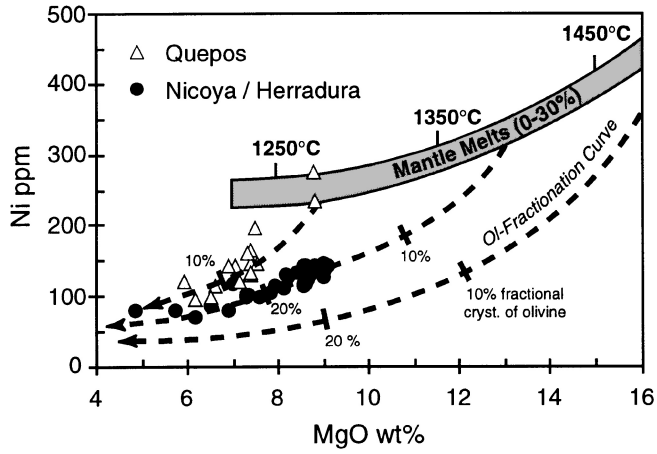

Fig. 6 Ni versus MgO for Nicoya, Herradura and Quepos tholeiites. The different trends imply derivation from parental melts with different MgO contents (and thus different temperatures) through olivine fractionation. Field for primary mantle melts and olivine fractionation curves after Hart and Davis (1978) and Nabelek and Langmuir (1986). Melting temperatures are from Hirose and Kushiro (1993)

cessation of melting will both result in a shorter melting column for Quepos and thus lower overall degrees of melting, as is also indicated by the higher abundances of incompatible elements in Quepos basalts (Fig. 4).

A Hotspot origin for Costa Rican terranes

As noted previously, the origin of Costa Rican oceanic terranes is controversial. For example, tholeiites from Nicoya alone have been interpreted to have formed in every possible tectonic setting (convergent, divergent and intra-plate). In this section, we show that plume-related volcanism in an intra-plate setting is the most likely origin of the studied terranes.

Interpretation of the Quepos terrane is the most straightforward, since all of the available data point to a hotspot origin. This includes 1) the lithostratigraphy of the Quepos terrane, indicating an evolution from seamount to ocean island, (3) petrological data implying a lithospheric thickness in excess of 16 km 3) lack of subduction-zone trace-element characteristics, e.g. relative depletion in Nb and Ta, and 4) trace-element and radiogenic-isotope characteristics of ocean islands.

The origin of the Nicoya/Herradura complexes is less straightforward. At first glance, several observations seem to suggest formation of Nicoya and Herradura magmas at a mid ocean ridge: 1) eruption of lavas in relatively deep water, 2) concentrations of incompatible elements similar (but not identical) to MORB, 3) lack of evidence for significant seafloor morphology, 4) tholeiitic composition and 5) shallow depths (<16 km) of differentiation. Nevertheless, the isotope data and more careful consideration of the major and trace element data show that formation at a mid ocean ridge is unlikely (Figs. 4, 7, 8, 10).

Comparison of the most mafic Nicoya and Herradura tholeiites to East Pacific Rise (EPR) tholeiites with similar MgO suggests that the melting conditions were generally different. As is shown in Figures 7 and 8, the Nicoya and Herradura tholeiites have lower abundances of Al_2O_3, Na_8 and incompatible elements such as Ti, Zr, Y and HREE but higher Fe_8 than the majority of EPR tholeiites. Lower Na_8 and incompatible-element concentrations in the Nicoya and Herradura tholeiites most likely reflect higher degrees of melting than for EPR tholeiites (Klein and Langmuir, 1987; Langmuir et al., 1992). Higher Fe_8 results from melting at greater average depth and/or of a more fertile source. Taken together, larger degrees of melting at greater average depth imply higher initial melting temperatures for Nicoya/Herradura as compared to EPR and most other MORB. The inferred melting temperatures of $1380 \pm 20\,^{\circ}C$ for Nicoya/Herradura are higher than temperatures generally proposed for the formation of MORB ($1280\,^{\circ}C$–$1350\,^{\circ}C$) (e.g. Klein and Langmuir, 1987, Kinzler and Grove, 1992, Langmuir et al., 1992). Higher temperatures in the Costa Rican source than in most MORB sources may reflect the involvement of anomalous hot mantle in the generation of these magmas.

Alternatively, these major and trace element differences could reflect a source with a composition distinct from most MORB, as is suggested by Figure 5. At similar pressures (i.e. SiO_2), the Nicoya, Herradura and Quepos lavas have higher FeO* than the experimental melts of Hirose and Kushiro (1993), indicating derivation from a more fertile or Fe-rich source (with

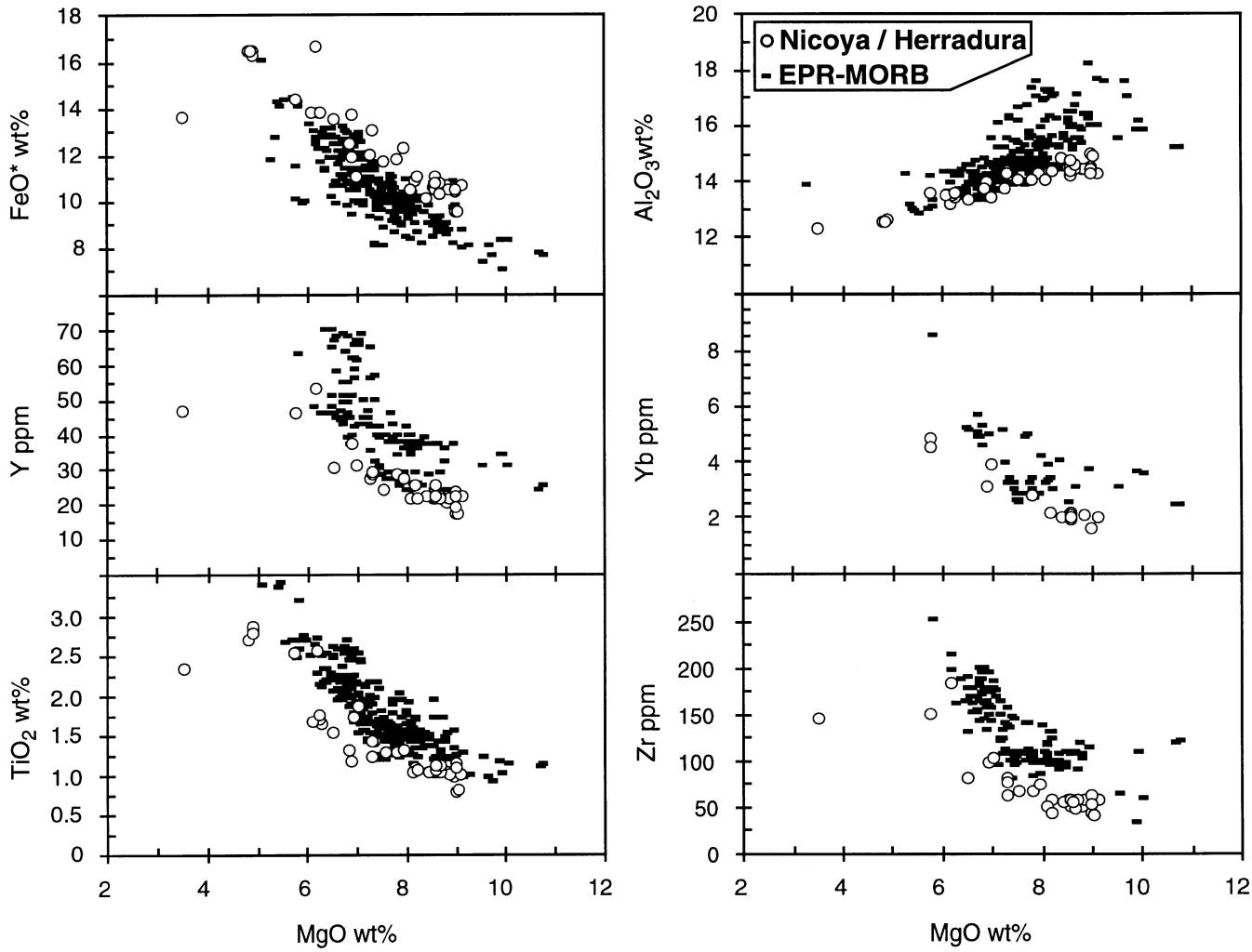

Fig. 7 Representative major and trace element abundances of Nicoya/Herradura tholeiites compared with East Pacific Rise (EPR) MORB from 23 °S–8 °N. EPR data from Natland and Melson (1980), Puchelt and Emmermann (1983) and Sinton et al. (1991). Only samples without Fe–Ti oxides were included in the MORB field

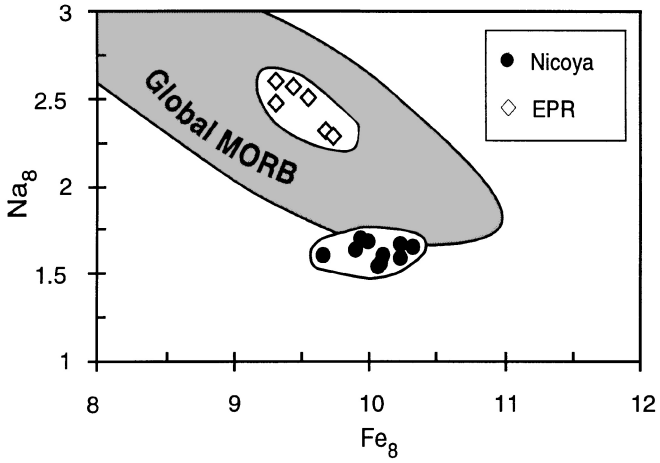

Fig. 8 Na_8 (Na at MgO = 8) and Fe_8 (Fe at MgO = 8) of basalt glasses from Nicoya compared to typical values for EPR and the global MORB array from Klein and Langmuir (1987). Nicoya tholeiites plot at the low Na_8 (high Fe_8) end of the global ridge array, reflecting larger degrees of melting over a longer melt column than for most MORB

forsterite content of <85) than is generally proposed for MORB. In summary, higher temperatures and/or more fertile source material are both compatible with the involvement of a mantle plume in the generation of Nicoya and Herradura tholeiites. The strongest evidence for a hotspot origin for Nicoya and Herradura, however, comes from the Sr-Nd-Pb isotope data (Fig. 10), which is distinct from MORB but falls within the range for oceanic island basalts, as was also the case for Quepos.

The Galápagos connection

Plate tectonic reconstructions show that the Central American oceanic terranes could have been derived from the Galápagos plume during the Cretaceous (Flüh, 1983; Duncan and Hargraves, 1984). Incompatible-element patterns (e.g. REE in Fig. 9) and Sr-Nd-Pb isotope data (Fig. 10a, b) from the Costa Rican terranes

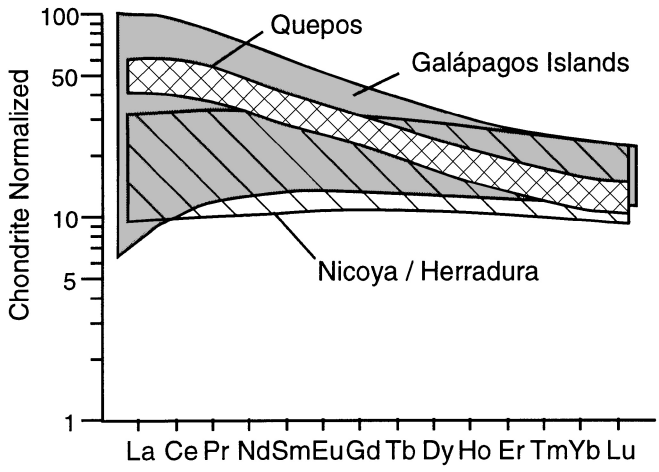

Fig. 9 Ranges of chondrite-normalized REE patterns for basalts from the Galápagos Islands (White et al., 1993) are compared with REE data from Nicoya, Herradura and Quepos tholeiites

are similar to volcanic rocks from the Galápagos Islands (White et al., 1993), consistent with this hypothesis. Nevertheless, the large variation in trace element concentrations in Galápagos lavas is thought to reflect plume/ridge interaction (White et al., 1993), whereas we interpret differences in trace element concentrations between Quepos and Nicoya/Herradura melts to result from melting over different depth intervals, ultimately reflecting different mantle temperatures and lithospheric thicknesses. Therefore the similar range in incompatible elements may be fortuitous.

Several additional pieces of data support a possible Galápagos connection. The Quepos complex (66 Ma) has been shown to be an accreted ocean island which must have been derived from a source in the Pacific. The geochemical data is consistent with derivation of Nicoya/Herradura from the same source. Paleomagnetic studies of these terranes (Frisch et al., 1992; Di Marco et al., 1994) show 1) that the Costa Rican terranes must have formed approximately 10° south of their present locations at an equatorial latitude and 2) that they have not been rotated relative to South America since their formation. These data provide further confirmation for a Galápagos origin.

In summary, the volcanological, petrological, geochemical and paleomagnetic data from the Costa Rica igneous terranes, combined with plate tectonic reconstructions of this region, indicate that the Galápagos source has been present for at least 90 Ma. Nevertheless, due to the ~50 Ma gap between the present Galápagos track (Fig. 1), consisting of the Cocos,

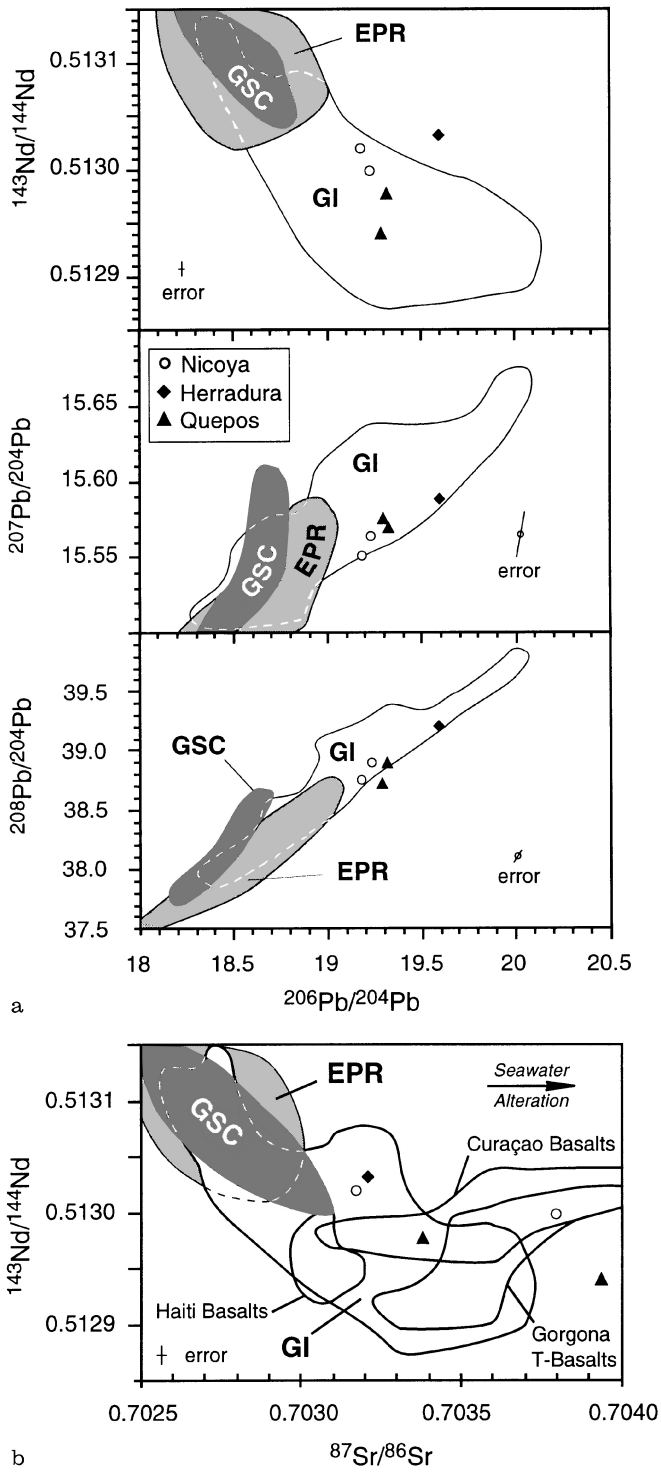

Fig. 10a Isotope correlation diagrams of $^{206}Pb/^{204}Pb$ versus $^{143}Nd/^{144}Nd$, $^{207}Pb/^{204}Pb$ and $^{208}Pb/^{204}Pb$, versus for Nicoya, Herradura and Quepos tholeiites. Tholeiites ar formed by relatively high degrees of melting, therefore parent/daughter ratios in the melts will be similar to those in the source. As a result, measured isotope ratios will be similar to the isotopic composition of the source at the present time and can be directly compared with young volcanic rocks from the Galápagos Islands (GI), the Galápagos Spreading Center (GSC) and East Pacific Rise (EPR) MORB (White et al. 1993) **b** Isotope correlation diagram for $^{87}Sr/^{86}Sr$ versus $^{143}Nd/^{144}Nd$. In addition to data from the Costa Rican terranes and the fields shown in Fig. 10b, fields for Haiti (Sen et al. 1988), Curaçao (Kerr et al. 1996b) and Gorgona (Echeverría 1980) tholeiites are also shown

Malpelo and Coiba Ridges (10–20 Ma) and the Costa Rican terranes (66–90 Ma), we can only speculate as to whether the present Galápagos plume has been continuously active for the past 90 Ma or whether the Costa Rican terranes were formed by a Galápagos precursor (Hauff et al., 1996).

Relationship of Costa Rican terranes to the Caribbean large igneous province

We have shown that the Nicoya, Herradura and Quepos terranes may represent part of the Galápagos plume activity between ~66–90 Ma. Basalts with similar geochemistry and age (~90 Ma) are reported from various parts of the Caribbean Plate, including Haiti, the Caribbean basement, Colombia, Ecuador and Curaçao (Donelly et al., 1973; Echeverría, 1980; Aitken and Echeverría, 1984; Dupré and Echeverría, 1984; Sen et al., 1988; Sinton et al. 1993; Hergt et al., 1994; Kerr et al., 1996a, b). Nd and Pb isotopic ratios from Gorgona, Haiti and Curaçao show a similar narrow compositional range. The larger variations in the Sr isotope ratio may reflect seawater alteration (Fig. 10b). Incompatible trace-element contents (e.g. chondrite-normalized REE patterns) of basalts from all these regions are similar to those of the Nicoya and Herradura tholeiites. Therefore the similarities in isotope, trace-element and age data strongly suggest a common mantle source region for these scattered volcanic areas. The occurrence of komatiites on Gorgona and picrites in Curaçao and Costa Rica is attributed to mantle 200–300 °C hotter than ambient upper mantle and has been linked to the presence of a mantle plume during their formation (Echeverría, 1980; Aitken and Echeverría, 1984; Kerr et al., 1966a, b; Alvarado, in prep.). The above observations have led to the concept of the Caribbean Plate, which has an aerial extent of ~1300 km by 2700 km and an anomalous crustal thickness of 10–15 km, being a large igneous province formed in the Mid Cretaceous (Burke, 1988, Storey et al., 1991, Hill, 1993).

Experimental work shows that starting plumes from the core-mantle boundary will have large heads (up to 1200 km in diameter), which can flatten to about twice their original diameter when they approach the base of the overlying lithosphere (Campbell and Griffiths, 1990; Griffiths and Campbell, 1990). Elongation of starting plume heads can result through asthenospheric flow and/or lithospheric drag (Griffiths and Campbell, 1991). The dimensions of the Caribbean plate are consistent with decompression melting of a flattened, elongated starting plume head, consistent with formation of the Caribbean Plate ~90 Ma ago by the Galápagos starting plume head (Hill, 1993). Evidence for a lower mantle origin for the Galápagos Plume comes from He isotopic data obtained from lavas of the Galápagos plateau (Graham et al., 1993).

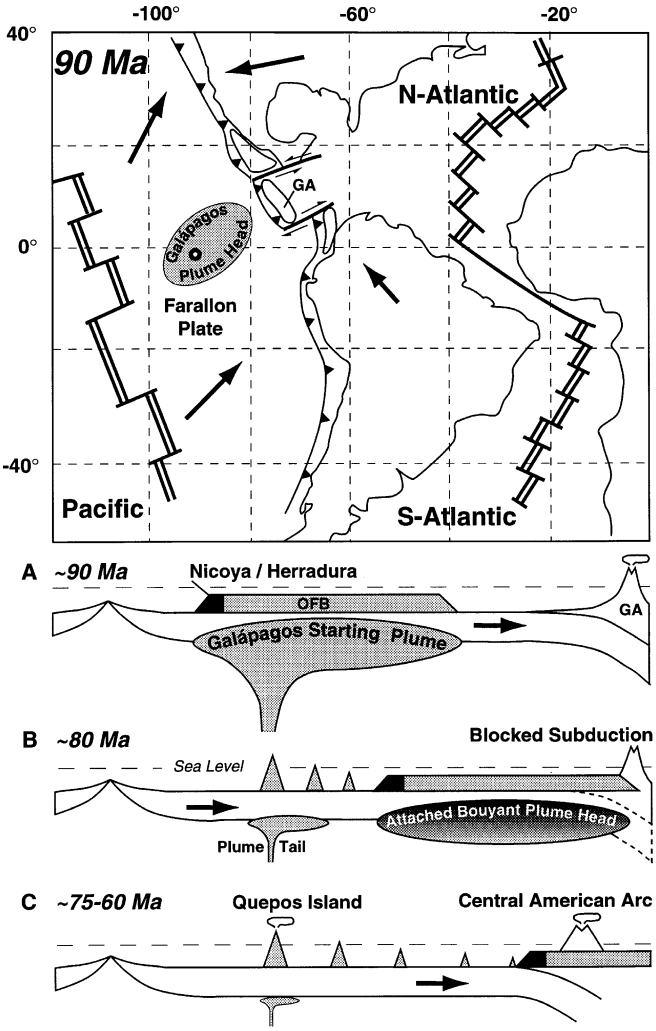

Fig. 11 The map schematically shows the plate configuration at 90 Ma after Duncan and Hargraves (1984). The cross sections below the map summarize the results of this study and combine them with the plate tectonic reconstructions of Duncan and Hargraves (1984) and the plume head model of Hill (1993). **A** The Nicoya/Herradura complexes are formed 90 Ma ago along the western margin of the Caribbean oceanic flood basalt province (OFB), generated by the head of the Galápagos starting plume. **B** The thickened, buoyant crust to which the hot plume head was attached caused a reverse in polarity of subduction at ~80 Ma. The Caribbean plate was formed when the Farallon and Atlantic plates began subducting along the western and eastern margins. Northeastward motion of the Caribbean plate moved the starting plume head away from the plume tail. **C** Melting of the plume tail formed Quepos Island about 66 Ma ago. Sometime thereafter Quepos was accreted to the Pacific margin of Central America

The location of Nicoya and Herradura on the Caribbean Plate, i.e. formation through volcanism associated with the plume head, could explain why these terranes have trace element characteristics similar to oceanic plateaus and why their REE concentrations extend to lower values than basalts from the Galápagos. Eruption of the Nicoya/Herradura tholeiites as flood basalts on pre-existing oceanic crust

could also explain the observed thermal overprinting of radiolarites and enigmatic biostratigraphic ages (Schmidt-Effing, 1979; Gursky, 1994) older than 90 Ma. In accordance with the model of Duncan and Hargraves (1984) (Fig. 11), the Caribbean large igneous province moved northeastwardly after formation. Due to its anomalous thickness and greater bouyancy, the plateau blocked subduction along the Greater Antilles arc, until there was a reverse in the polarity of subduction which resulted in the subduction of normal Atlantic oceanic crust ($\sim$7 km thick). Oceanic terranes in Columbia, Ecuador, Panama and Costa Rica (e.g. Nicoya and Herradura) were either obducted along the South American continental margin or uplifted when subduction of normal Pacific oceanic crust began around 75 Ma as indicated by arc-derived sediments (e.g. the Sabana Grande Formation which covers the Nicoya and Herradura terranes discordantly). Seamounts and ocean islands (e.g. Quepos), which formed from the Galápagos plume tail, were subsequently accreted along the western margin of the Caribbean plateau. Evidence for the occurrence of ocean islands (such as Quepos) in the Eastern Equatorial Pacific as far back as 66 Ma may extend the speciation time for Galápagos biota from a common gene pool much further than previously thought (Christie et al., 1992). Together with subduction-zone volcanism, these accreted volcanic edifices formed the Central American isthmus connecting North and South America (Fig. 11).

Conclusions

The present study integrates volcanological, petrological and geochemical data from three oceanic crustal segments in Costa Rica into a coherent petrogenetic and tectonic model. We have shown that:

1) The Quepos terrane represents a drowned oceanic island that was subsequently accreted to Central America. The Nicoya and Herradura terranes consist of oceanic plateau-forming tholeiites. No volcanic facies or geochemical differences exist between north and south Nicoya.
2) Quepos transitional tholeiites evolved through fractional crystallisation of ol + cpx $\pm$ Cr-spinel in deep-seated magma chambers at greater than 16 km depth. Nicoya/Herradura tholeiites, on the other hand, developed through fractionation of ol + plag $\pm$ Cr-spinel at less than 16 km depth. These differences may reflect thicker lithosphere beneath Quepos.
3) Sr-Nd-Pb isotopic data indicate a common mantle source for Nicoya, Herradura and Quepos, despite their different ages. Major and trace element data indicate that Quepos tholeiites formed by lower degrees of melting at lower temperatures but greater average depth than Nicoya/Herradura tholeiites.
4) Volcanological, petrological, geochemical and age data are consistent with Nicoya/Herradura complexes forming part of a Mid-Cretaceous flood basalt province generated by the head of the Galápagos starting plume, implying a 90 Ma age for th Galápagos hotspot. The Quepos terrane appears to represent the oldest known seamount/ocean island formed by melting of the Galápagos plume tail.

Acknowledgements Reviews by Colin Devey and an anonymous reviewer significantly improved the manuscript. Guillermo Alvarado (Costa Rica) kindly provided valuable information and very helpful logistical support in the field. Antje Merkau carried out XRF analyses at GEOMAR. Jürgen Freitag and Petra Glöer (GEOMAR) assisted with microprobe work. Dieter Garbe-Schnöberg and Tom Arpe carried out ICP-MS analyses. We are grateful to George Tilton for providing K.H. with access to his isotope facilities and for generously analyzing several samples for Sr isotopic composition at no cost. F.H. thanks Chris Sinton for providing him with a preliminary copy of one of his dissertation chapters while this manuscript was being prepared. The study was supported by the Deutsche Forschungsgemeinschaft (Grant Schm 250/59-1: TICOSECT/Terranes).

References

Aitken BG, Echeverría LM (1984) Petrology and geochemistry of komatiites and tholeiites from Gorgona island, Colombia. Contrib Mineral Petrol 86:94–105

Albarede F, Tamagnan V (1898) Modelling the recent geochemical evolution of the Piton de la Fournaise Volcano, Réunion Island, 1931–1986. J Petrol 29:997–1030

Alvarado GE, Kussmaul S, Chiesa S, Gillot P-Y, Appel H, Wörner G, Rundle C (1992) Resumen chronostratigráphico de las rocas igneas de Costa Rica basado en dataciones radiométricas K-Ar y U-Th. J South Am Earth Sci 6:151–168

Baumgartner PO, Mora CR, JB, Sigal J, Glacon G, Azéma J, Bourgois J (1984) Sedimentacion y paleogeografia del Cretacico y Cenozoico del litoral Pacifico de Costa Rica. Rev Geol Am Centr 1:57–136

Burke K (1988) Tectonic evolution in the Caribbean. Ann Rev Earth Planet Sci 16:201–230

Campbell IH, Griffiths RW (1990) Implications of mantle plume structure for the evolution of flood basalts. Earth Planet Sci Lett 99:79–93

Chaffey DJ, Cliff RA, Wilson BM (1989) Characterization of the St Helena magma source. In: Saunders AD, Norry MJ (eds) Magmatism in the ocean basins. Spec Publ Geol Soc Lond 42:257–276

Christie DM, Duncan RA, McBirney AR, Richards MA, White WM, Harpp KS, Fox CG (1992) Drowned islands downstream from the Galápagos hotspot imply extended speciation times. Nature 355:246–248

Coleman RG (1977) Ophiolites. Springer, Berlin Heidelberg New York, pp 1–229

Devey CW, Garbe-Schönberg CD, Stoffers P, Chauvel C, Mertz DF (1994) Geochemical effects of dynamic melting beneath ridges: reconciling major and trace element variations in Kolbeinsey (and global) mid-ocean ridge basalt. J Geophys Res 99:9077–9095

Di Marco G, Baumgartner PO, Channel JET (1995) Late Cretaceous-early Tertiary paleomagnetic data and a revised tectonostratigraphic subdivision of Costa Rica and western Panama. In: Mann P (ed) Geologic and tectonic development of the Caribbean plate boundary in southern Central America. Geol Soc Am Spec Pap 295:1–27

Donelly TW, Melson W, Kay R, Rogers JJW (1973) Basalts and dolerites of late Cretaceous age from the Central Caribbean. In: Init Rpts Deep Sea Drilling Proj 15:989–1012

Donnelly TW, Beets D, Carr MJ, Jackson T, Klavier G, Lewis J, Maury R, Schellenkens H, Smith AL, Wadge G, Westercamp D (1990) History and tectonic setting of Caribbean magmatism. In: Dengo G and Case JE (ed) The Geology of North America, Vol H: The Caribbean Region, Geological Society America, Boulder, Colo.: 339–374

Duncan RA, Hargraves RB (1984) Caribbean region in the mantle reference frame. In: Bonini W, Hargraves RB, Shagam, R (eds) The Caribbean-South American plate boundary and regional tectonics. Geol Soc Am Mem 162 : 89–121

Dupré B, Echeverría LM (1984) Pb isotopes of Gorgona island (Colombia): isotop variations correlated with magma type. Earth Planet Sci Lett 67 : 186–190

Echeverría LM (1980) Tertiary or Mesozoic komatiites from Gorgona island, Colombia: field relations and geochemistry. Contrib Mineral Petrol 73 : 253–266

Flüh E (1983) The basic igneous complex – Trace of an ancient Galápagos hotspot aseismic ridge? Zbl Geo Paläont 3/4 : 291–303

Frisch W, Meschede M, Sick M (1992) Origin of the Central American ophiolites: evidence from paleomagnetic results. Geol Soc Am Bull 104 : 1301–1314

Galli-Olivier C (1979) Ophiolite and island arc volcanism in Costa Rica. Geol Soc Am Bull 90 : 444–452

Garbe-Schönberg C-D (1993) Simultaneous determination of thirty-seven trace elements in twenty-eight international rock standards by ICP-MS. Geostand Newslett 17 : 81–97

Govindaraju K (1994) Compilation of working values and sample descriptions for 383 geostandards. Geostand Newslett 18 : 1–158

Graham DW, Christie DM, Harpp KS, Lupton JE (1993) Mantle plume helium in submarine basalts from the Galápagos platform. science 262 : 2023–2026

Griffiths RW, Campbell IH (1990) Stirring and structure in mantle plumes. Earth Planet Sci Lett 99 : 66–78

Griffiths RW, Campbell IH (1991) On the dynamics of long-lived plume conduits in the convecting mantle. Earth Planet Sci Lett 103 : 214–227

Gursky H-J (1994) The oldest sedimentary rocks of South Central America: the radiolarian cherts of the Nicoya Ophiolite Complex (?Early Jurassic to Late Cretaceous). Profil 7 : 265–277

Hart SR, Davis KE (1978) Nickel partitioning between olivine and silicate melt. Earth Planet Sci Lett 40 : 203–219

Hauff F, Hoernle K, Werner R, Schmincke H-U (1996) Origin of the central american ophiolites through plume/ridge interaction. J Conf Abstr 1(1) : 238

Hémond C, Hofmann AW, Heusser G, Condomines M, Raczek I, Rhodes JM (1994) U-Th-Ra systematics in Kilauea and Mauna Loa basalts, Hawaii, Chem Geol 116 : 163–180

Hergt JM, Storey M, Marriner G, Tarney J (1994) The Curaçao lava formation: samples of the oldest and most primitive magmas from the Galápagos plume. Mineral Mag 58 : 414–415

Hill RI (1993) Mantle plumes and continental tectonics. Lithos 30 : 193–206

Hinz K, Huene Rv, Ranero CR, Group PW (1996) Tectonic structure of convergent Pacific margin offshore Costa Rica from multichannel seismic reflection data. Tectonics 15 : 54–66

Hirose K, Kushiro I (1993) Partial melting of dry peridotites at high pressures: determination of compositions of melts segregated from peridotite using aggregates of diamond. Earth Planet Sci Lett 114 : 477–489

Hoernle KA, Schmincke H-U (1993) The role of partial melting in the 15-Ma geochemical evolution of Gran Canaria: a blob model for the Canary hotspot. J Petrol 34 : 599–626

Hoernle KA, Tilton G, Schmincke H-U (1991) Sr-Nd-Pb isotopic evolution of Gran Canaria: evidence for shallow enriched mantle beneath the Canary Islands. Earth Planet Sci Lett 106 : 44–63

Hoernle KA, Tilton GR (1991) Sr-Nd-Pb isotope data for Fuerteventura (Canary Islands) basal complex and subaerial volcanics: applications to magma genesis and evolution. Schweiz Mineral Petrogr Mitt 71 : 3–18

Hofmann AW, Jochum KP, Seufert M, White WM (1986) Nb and Pb in oceanic basalts: new constraints on mantle evolution. Earth Planet Sci Lett 79 : 33–45

Huene Rv, Bialas E, Flühl E, Cropp B, Csernok T, Fabel E, Hoffmann J, Emeis K, Holler P, Jeschke G, Leandro C, Peréz Fernandéz I, Chavarria S, Florez A, Escobedo Z, Léon R, Barrios O (1995) Morphotectonics of the Pacific convergent margin of Costa Rica. In: Mann P (ed) Geologic and tectonic development of the Caribbean plate boundary in southern Central America. Geol Soc Am Spec Pap 295 : 291–307

Kerr AC, Tarney J, Marriner GF, Klaver GT, Saunders AD, Thirlwall MF (1996a) The geochemistry and petrogenesis of the late-Cretaceous picrites and basalts of Curaçao, Netherlands Antilles: a remnent of an oceanic plateau. Contrib Mineral Petrol 124 : 29–43

Kerr AC, Marriner GF, Arndt NT, Tarney J, Niva A, Saunders AD, Duncan RA (1996b) The petrogenesis of Gorgona komatiites, picrites and basalts: new field, petrographic and geochemical constraints. Lithos 37 : 245–260

Kinzler RJ, Grove TL (192) Primary magmas of mid-ocean ridge basalts 2. applications. J Geophys Res 97 : 6907–6926

Klein EM, Langmuir CH (1987) Global correlations of ocean ridge basalt chemistry with axial depth and crustal thickness. J Geophys Res 92 : 8089–8115

Langmuir CH, Klein EM, Plank T (1992) Petrological systematics of mid-ocean ridge basalts: constraints on melt generation beneath ocean ridges. In: Morgan JP, Blackman DK and Sinton JM (ed) Mantle flow and melt generation at mid-oceanic ridges. Am Geophys Union Monograph 781 : 183–280

Mann P (1995) Geologic and tectonic development of the Caribbean plate boundary in southern Central America. Geol Soc Am Spec Pap 295 : 1–349

Moore JG, Schilling JG (1973) Vesicles, water and sulfur in Reykjanes Ridge basalts. Contrib Mineral Petrol 41 : 105–118

Nabelek PI, Langmuir CH (1986) The significance of unusual zoning in olivines from FAMOUS area basalt 527-1-1. Contrib Mineral Petrol 93 : 1–8

Natland JH, Melson WG (1980) Composition of basaltic glasses from the East Pacific Rise and Siqueiros fracture zone, near 9 °N. Init Rpts Deep Sea Drilling Proj 54 : 705–723

Puchelt, Emmermann R (1983) Petrogenetic implications of tholeiitic basalt glasses from the East Pacific Rise and the Galápagos spreading center. Chem Geol 38 : 39–56

Schmidt-Effing R (1979) Alter und Genese des Nicoya-Komplexes, einer ozeanischen Paläokruste (Oberjura bis Eozän) im südlichen Zentralamerika. Geol Rundsch 68 : 457–494

Sen G, Hickey-Vargas R, Waggoner DG, Maurasse F (1988) Geochemistry of basalts from the Dumisseau Formation, southern Haiti: implications for the origin of the Caribbean Sea crust. Earth Planet Sci Lett 87 : 423–437

Sinton CW, Duncan RA, Storey M (1993) ^{40}Ar-^{39}Ar ages from Gorgona Island, Columbia and the Nicoya Peninsula, Costa Rica. EOS 74 : 553

Sinton JM, Smaglik SM, Mahoney JJ (1991) Magmatic processes at superfast spreading mid-ocean ridges: glass compositional variations along the East Pacific Rise 13°–23°. J Geophys Res 96 : 6133–6155

Storey M, Mahoney JJ, Kroenke LW, Saunders AD (1991) Are oceanic plateaus sites of komatiite formation? Geology 19 : 376–379

Sun S-S, McDonough WF (1989) Chemical and isotopic systematics of oceanic basalts: implications for mantle composition and processes. In: Saunders AD, Norry MJ (eds) Magmatism in the ocean basis. Spec Publ Geol Soc Lond 42 : 313–345

Tournon J (1984) Magmatismes du Mésozoiques à l'Actuel en Amérique Centrale: L'exemple de Costa Rica, des ophiolites aux andésites. Mém Sci de la Terre, Université Pierre et Marie Curie, Paris (84–49): 1–335

White WM, McBirney AR, Duncan RA (1993) Petrology and geochemistry of the Galápagos Islands: portrait of a pathological mantle plume. J Geophys Res 98 : 19533–19563